Supplementary Information

Nickel-based Single-Atom Alloys for Methane Dehydrogenation and the Effect of Subsurface Carbon: First-principles Investigations

Naiyuan Dong,[1,2] Tanglaw Roman,[3,4] and Catherine Stampfl[1,2,*]

[1]*School of Physics, The University of Sydney, NSW 2006, Australia*

[2] *The University of Sydney Nano Institute, 2006, NSW, Australia,* * *corresponding author catherine.stampfl@sydney.edu.au*

[3]*Flinders Institute for Nanoscale Science and Technology, College of Science and Engineering, Flinders University, Bedford Park, SA 5042, Australia*

[4]*Flinders Microscopy and Microanalysis, Flinders University, Bedford Park, SA 5042, Australia*

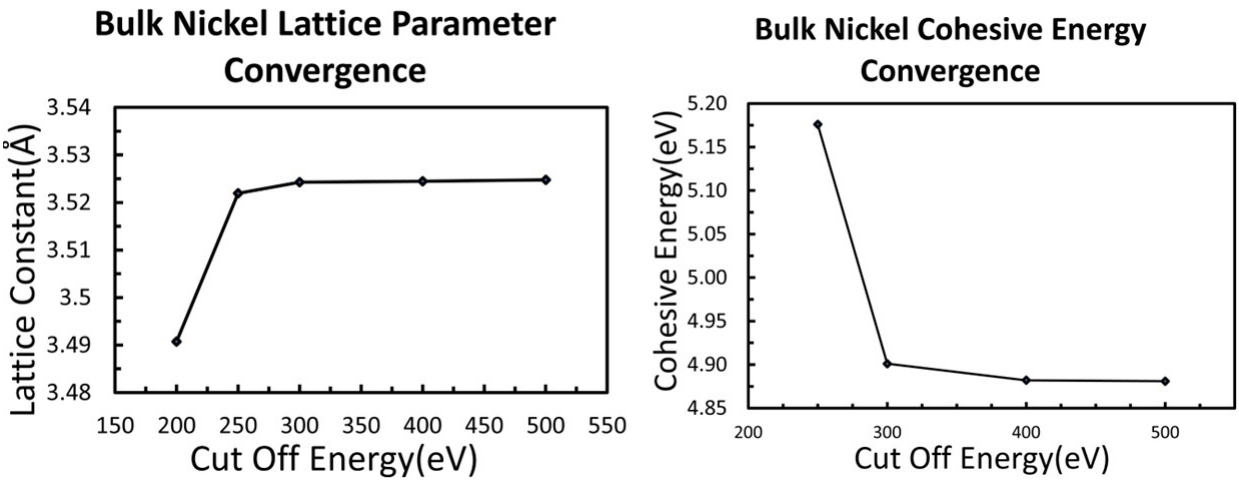

Figure 1. Convergence test of the bulk nickel lattice constant (left) and cohesive energy (right) for different cutoff energies using a **k**-point mesh of 9 × 9 × 9.

A. Convergence tests

To determine appropriate parameters to use in the calculations, it is mandatory to first test for the convergence of fundamental properties with varying the parameters used in the calculation. Convergence tests are carried out for the lattice parameter, cohesive energy and magnetic moment of the free Ni atom and bulk Ni for increasing energy cut-off and **k**-point mesh.

In Fig. S1 (left) the convergence behavior of the equilibrium lattice constant of nickel as a function of cut-off energy is shown, as calculated using a 9×9×9 **k**-point mesh. The lattice constant converges to a value of about 3.524 Å. In Fig. S1 (right) the convergence of the cohesive energy of bulk nickel as a function of cut-off energy is shown, also calculated using a 9×9×9 **k**-point mesh. The cohesive energy converges to a value of approximately 4.88 eV.

The convergence of the magnetic moment of the free atom and bulk Ni with increasing cut-off energy is shown in Fig. S2 left and right, respectively. The magnetic dipole moment of Ni in the bulk system converges more slowly (converging to 2.37μ_B with 300 eV cut-off energy) than the single atom system (converging to 1.95 (μ_B) for 270 (eV)). Since the cutoff energy for which the cohesive energy converges is larger than the other quantities considered, we take the cut-off energy to be 450 eV to ensure the accuracy of the calculations.

The lattice parameter of bulk nickel, 3.524 Å, was determined by calculating the total

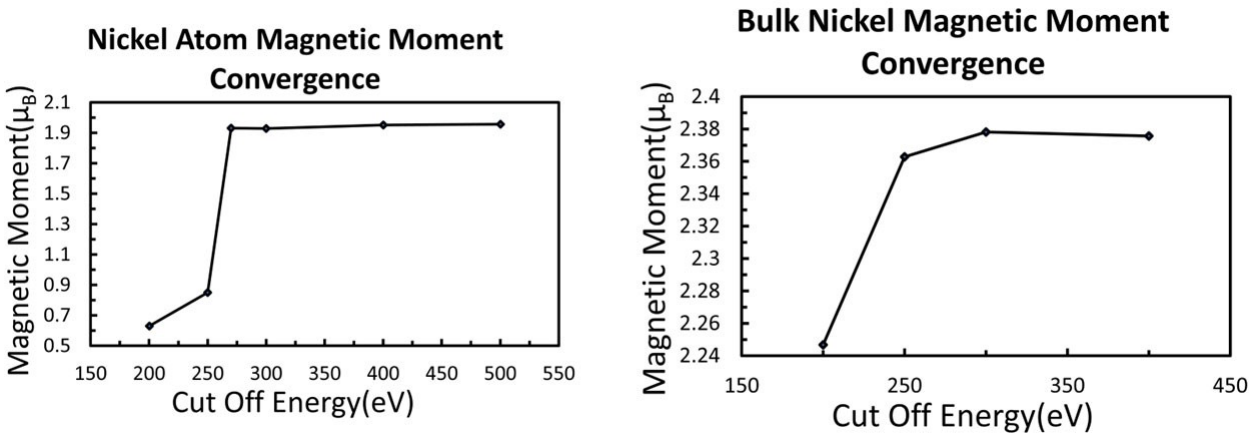

Figure 2. Convergence test for the magnetic moment of a free single nickel atom (left) calculated in a large box of 15 Å side length and the Gamma point for **k**-point sampling, and bulk nickel (right) for different cut-off energies using the gamma-point and a **k**-point mesh of 9 × 9 × 9, respectively.

energy for different lattice parameters over a range of 3.3 Å, to 3.7 Å, as shown in Fig. S3 (left) and fitted using a polynomial to obtain the minimum value. It is also mandatory to determine a sufficient vacuum region for the surface calculations. In Fig. S3 (right), the adsorption energy of a methane on (4 × 4)Ni(111) is shown as a function of vacuum region thickness. It can be seen that a vacuum region of 15 Å, yields sufficiently converged results, and is used for all calculations.

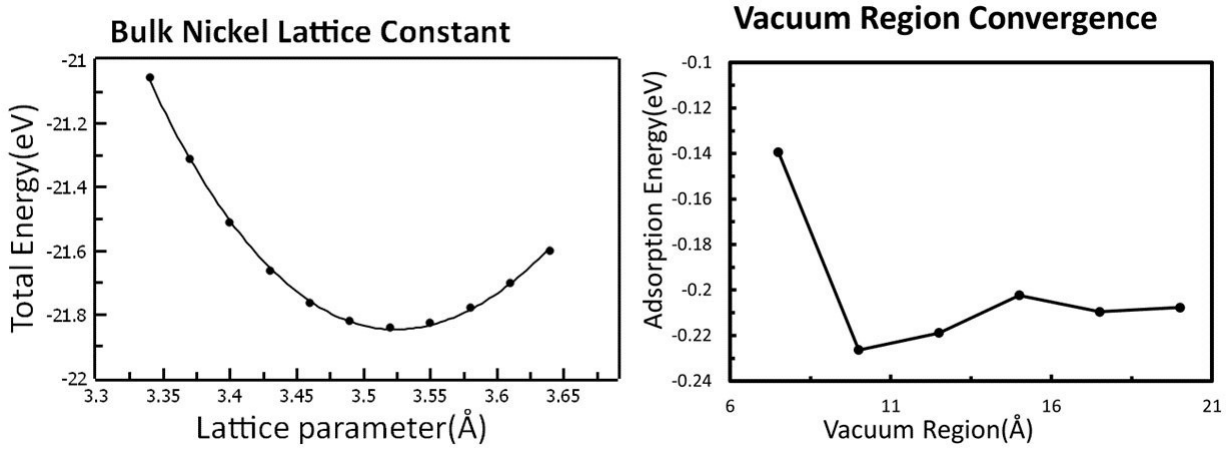

Figure 3. Example of curve fitting for the bulk nickel total energy for different lattice parameters using a **k**-point mesh of 9×9×9 and energy cutoff 450 eV (left), and the convergence of the relative adsorption energy of methane on (4 × 4)/Ni(111) in the on-top site for different vacuum regions using a **k**-point mesh of 9 × 9 and energy cutoff 450 eV.

To establish a sufficiently accurate **k**-point set for the Brillouin Zone (BZ) integration

several sized sets were considered. The **k**-point convergence test in Fig. S4 shows that the total energy of the Ni(111) surface system is fully converged with a 7 × 7 **k**-point set, as seen from Fig. 4 (left). We decided, to ensure the accuracy for the various alloy systems, to use a 9×9 **k**-point set.

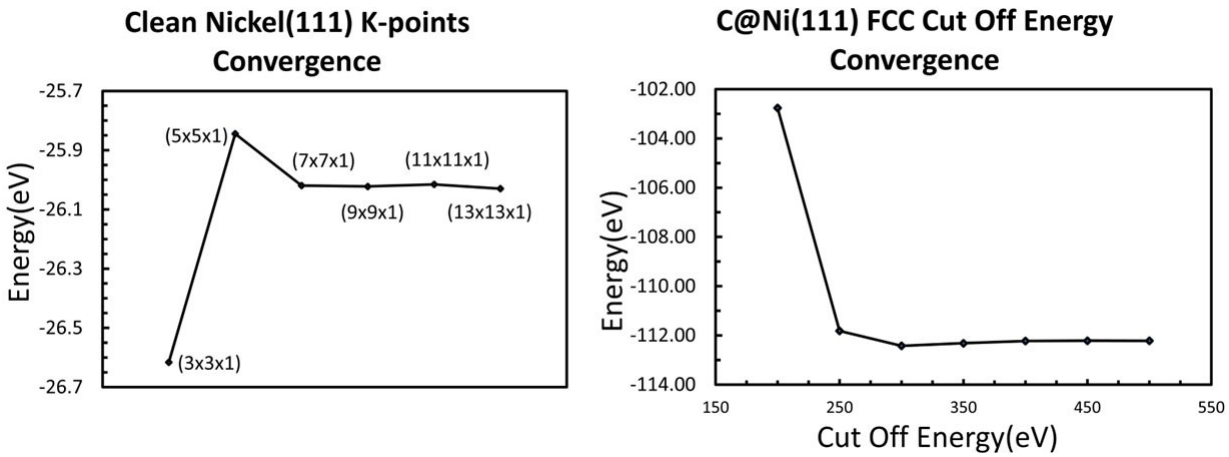

Figure 4. Convergence tests of the total energy of (1×1)-Ni(111) for different **k**-point sets (left) and that of (2×2)C-Ni(111) for C in the fcc hollow site as a function of energy cutoff, using a **k**-point mesh of 9 × 9. It can be seen from the latter that that the adsorption energy is well converged by 300 eV.

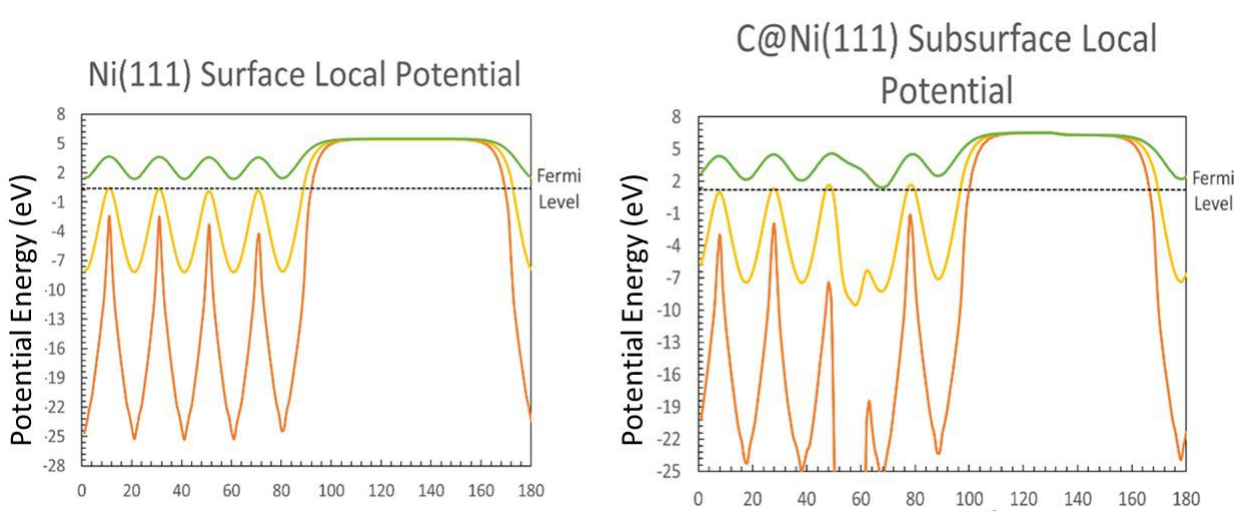

Figure 5. Electrostatic potential as function of position along the z-direction, with minimum (red), average (yellow) and maximum (green) for the clean Ni(111) surface (left) and the surface with subsurface C for 0.25ML (right). The horizontal dashed line is the position of the Fermi energy, and the vacuum energy corresponds to the energy in the center of the vacuum region. For the horizontal axis, a value of one corresponds to 0.23 Å along the direction perpendicular to the surface.

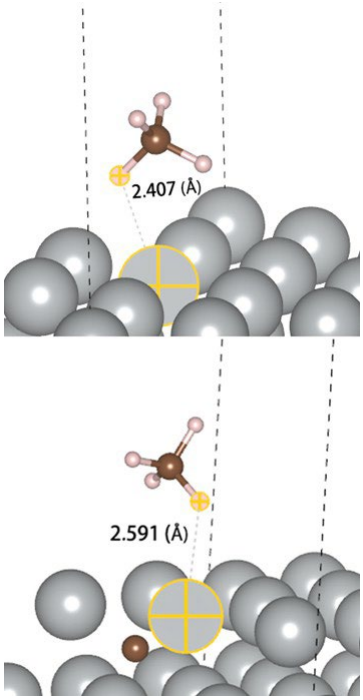

Figure 6. Bond lengths for methane on Ni(111) (upper) and the same but when there is a carbon atom in the subsurface site (lower).

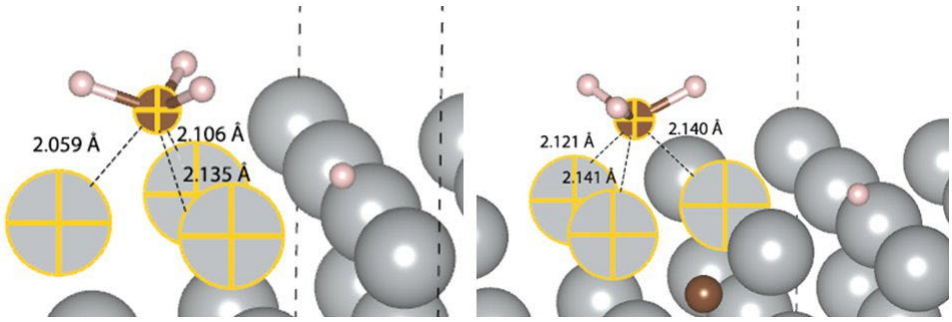

Figure 7. Bond lengths for CH_3 on Ni(111) (left) and the same but when there is a carbon atom in the subsurface site (right).

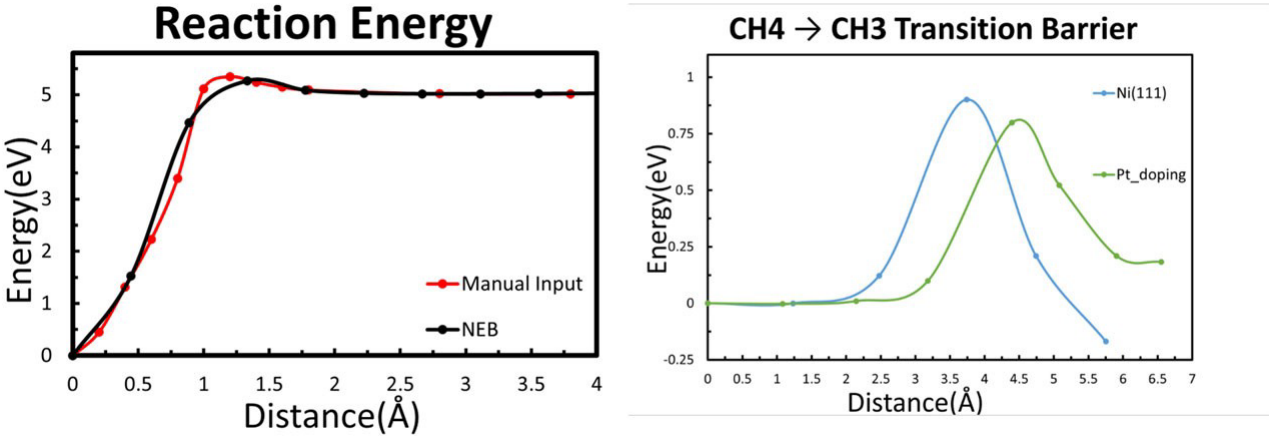

Figure 8. Left: Total energy for the reaction $CH_4 \rightarrow CH_3$+H by manually pulling one H away from CH_4 in vacuum and by calculation using the NEB VTST. Right: Example of the reaction barrier energy as calculated using the NEB VTST in VASP for $CH_4 \rightarrow CH_3$ + H over the clean Ni(111) surface (blue), and for doping with Pt (green).

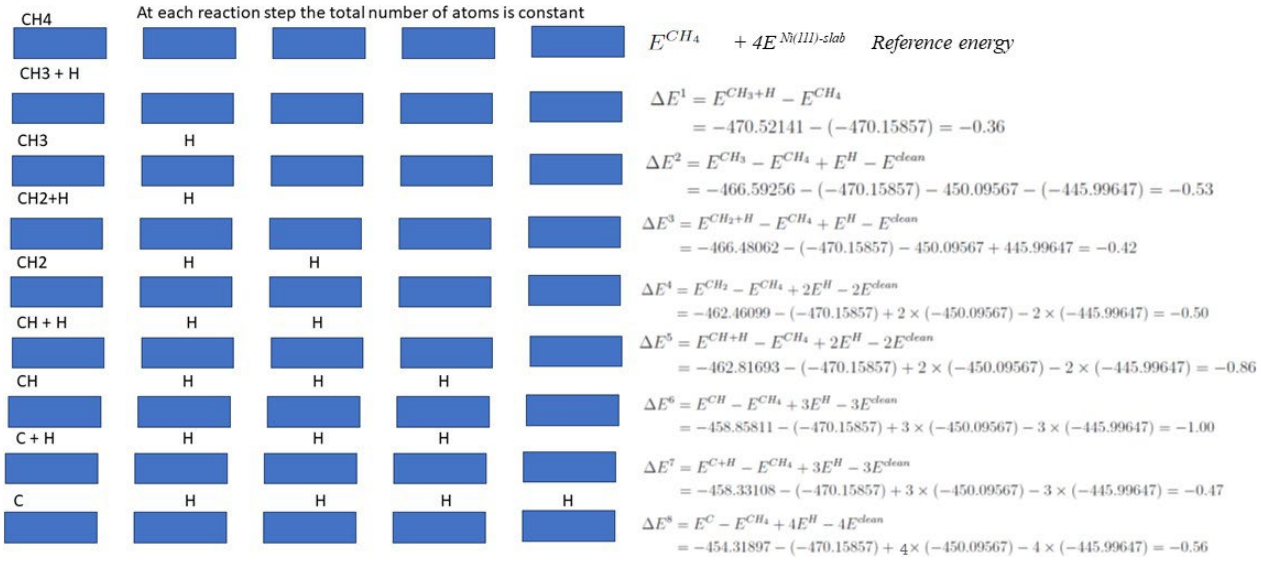

Figure 9. Schematic of calculation of energy diagram for maintaining same number of atoms at each reaction step and with a common reference energy. After dissociation of each H atom, it is taken that the H atom diffuses to an isolated position on the Ni(111) surface which ensures there are no adparticle-adparticle interactions. Otherwise this would affect the relative energy of the subsequent dissociation step. The energy zero is taken to be the total energy of the "*Reference energy*", methane adsorption on the surface plus four clean Ni(111) slabs.

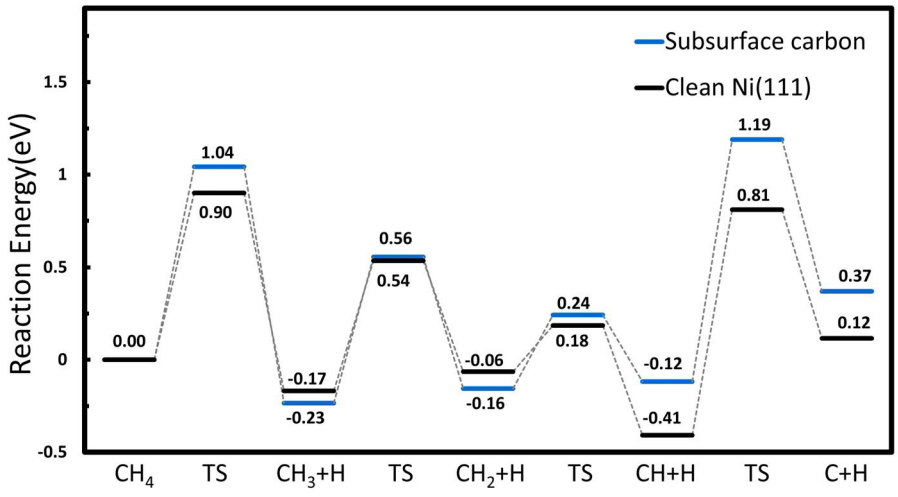

Figure 10. Energy diagram for methane dissociation over the Ni(111) surface (black lines) and this surface with a subsurface carbon atom (blue lines). The energy zero is the total energy of methane adsorbed on the respective surface. The energy barrier for reaction $CH_x \rightarrow CH_{x-1}$+H is plotted relative to the energy of the final state of the previous reaction, namely, CH_x+H, rather than to a common energy zero.

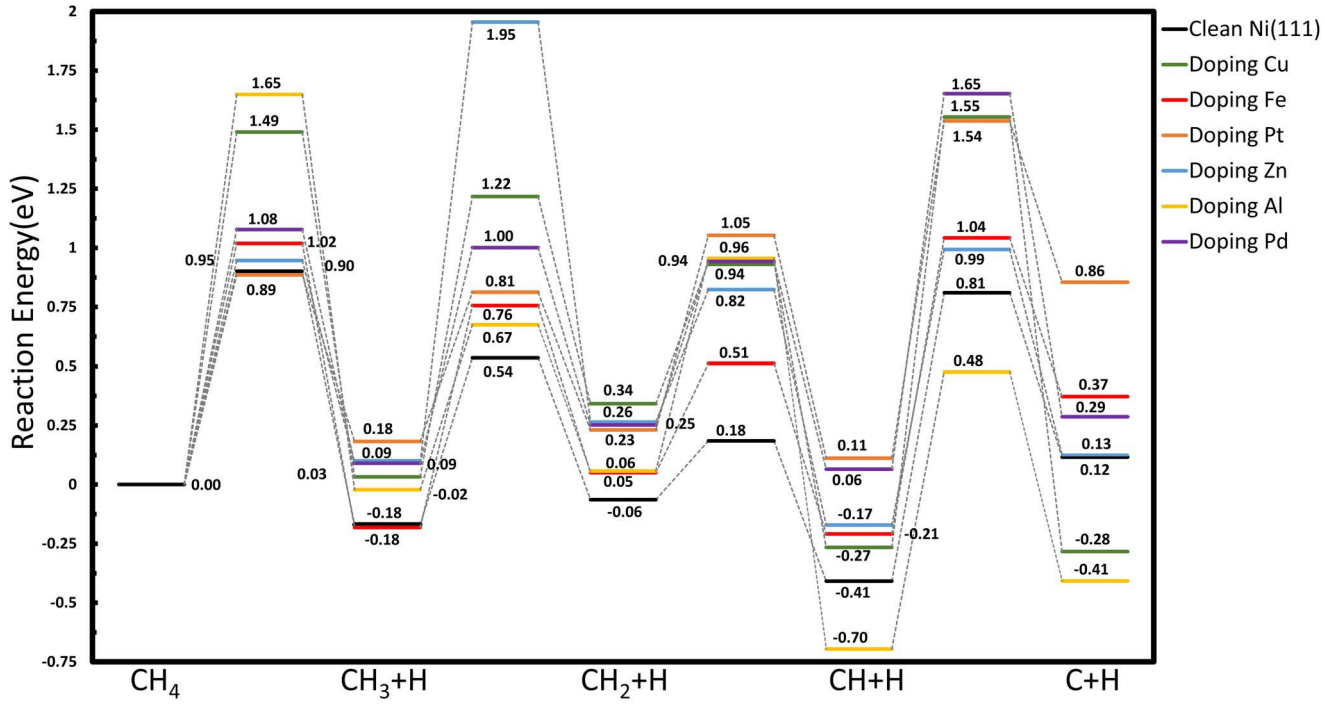

Figure 11. Energy diagram for methane dissociation over the SAA surfaces. The energy zero is the total energy of methane adsorbed on the SAA surface. The energy barrier for reaction $CH_x \rightarrow CH_{x-1}+H$ is plotted relative to the energy of the final state of the previous reaction, namely, CH_x+H, rather than to a common energy zero.